

A Minimal Input Engine Friction Model for Power Loss Prediction

Original

A Minimal Input Engine Friction Model for Power Loss Prediction / Delprete, Cristiana; Gastaldi, Chiara; Giorio, Lorenzo.
- In: LUBRICANTS. - ISSN 2075-4442. - 10:5(2022), p. 94. [10.3390/lubricants10050094]

Availability:

This version is available at: 11583/2972534 since: 2022-10-21T20:48:20Z

Publisher:

MDPI

Published

DOI:10.3390/lubricants10050094

Terms of use:

This article is made available under terms and conditions as specified in the corresponding bibliographic description in the repository

Publisher copyright

(Article begins on next page)



Real-Time Monitoring of Human and Process Performance Parameters in Collaborative Assembly Systems using Multivariate Control Charts

Elisa Verna¹ · Stefano Puttero¹ · Gianfranco Genta¹ · Maurizio Galetto¹

Received: 3 April 2023 / Accepted: 11 August 2024
© The Author(s) 2024

Abstract

With the rise in customized product demands, the production of small batches with a wide variety of products is becoming more common. A high degree of flexibility is required from operators to manage changes in volumes and products, which has led to the use of Human-Robot Collaboration (HRC) systems for custom manufacturing. However, this variety introduces complexity that affects production time, cost, and quality. To address this issue, multivariate control charts are used as diagnostic tools to evaluate the stability of several parameters related to both product/process and human well-being in HRC systems. These key parameters monitored include assembly time, quality control time, total defects, and operator stress, providing a more holistic view of system performance. Real-time monitoring of process performance along with human-related factors, which is rarely considered in statistical process control, provides comprehensive stability control over all customized product variants produced in the HRC system. The proposed approach includes defining the parameters to be monitored, constructing control charts, collecting data after product variant assembly, and verifying that the set of parameters is under control via control charts. This increases the system's responsiveness to both process inefficiencies and human well-being. The procedure can be automated by embedding control chart routines in the software of the HRC system or its digital twin, without adding additional tasks to the operator's workload. Its practicality and effectiveness are evidenced in custom electronic board assembly, highlighting its role in optimizing HRC system performance.

Keywords Statistical process control · Mass customisation · Human-robot collaboration · Industry 5.0

1 Introduction

In today's manufacturing environment, the number of product variants is constantly increasing due to the market-driven growth of customisation, which involves the production of small batches with a wide variety of products [1–3]. This trend is particularly evident in industries like electronics and automotive, where customisation ranges from hardware configurations to personalized features [4]. This trend towards mass customisation has also led to the development of new technologies, such as additive manufacturing and modular manufacturing. These technologies facilitate the cost-effective production of highly customised products [5, 6].

As a result, there has been a significant shift from mass production to the production of small batches, requiring high flexibility from operators. In mass customisation, the pairing of humans with collaborative robots, i.e. cobots, in so-called Human-Robot Collaboration (HRC) systems is proving effective [2, 7]. However, the complexity introduced by product variety impacts production time, cost, and quality [8]. Thus, managing this complexity in HRC systems used for customised production is critical [8].

Therefore, there is a need for effective monitoring of the multiple variables of the manufacturing process to ensure the stability of the production system and avoid critical situations and delays. To meet this need across various HRC applications, the paper proposes a flexible approach using Statistical Process Control (SPC) tools, particularly Multivariate Control Charts (MCCs). This method adapts to different contexts by incorporating a range of parameters specific to each application, including both process and human well-being metrics. In general, MCCs are used whenever simultaneous control of two or more quality

✉ Elisa Verna
elisa.verna@polito.it

¹ Department of Management and Production Engineering,
Politecnico di Torino, Corso Duca degli Abruzzi 24,
10129 Torino, Italy

characteristics is required [9]. The proposed approach exploits MCCs as diagnostic tools in evaluating the stability of several variables related to each product variant assembly concerning both process (i.e., process total defects, assembly and quality control times), and human well-being (i.e., human stress response). Real-time data are directly used for the diagnosis. A key feature of the proposed approach is the capability to monitor process performance jointly with human-related factors, which are seldom considered in SPC methods. Thus, in contexts where human-robot collaboration is key, and human well-being is as crucial as process performance, this approach is particularly suitable.

The approach proposed includes: (i) defining the parameters to be monitored; (ii) constructing control charts; (iii) collecting data after product variant assembly; (iv) verifying through control charts that the set of parameters is under control. If not, the causes of out-of-control data are identified in real-time and corrective action is taken to remove them and prevent their recurrence. The procedure can be automated by embedding MCCs routines in the software of the HRC system or its digital twin [10].

Thus, the proposed method aims to provide real-time feedback on system performance, enabling immediate identification of out-of-control situations and prompt corrective action, thus contributing significantly to achieving the goals of human-centred manufacturing in the Industry 5.0 paradigm.

This method is applied in this study to an HRC system for custom electronic board assembly, showcasing its adaptability. However, it can be extended to diverse contexts in HRC systems, as it effectively monitors both process and physiological parameters related to human operators. This flexible method thus contributes significantly to the goals of human-centered manufacturing in the Industry 5.0 paradigm.

The remainder of the paper is organized as follows. Section 2 presents a thorough review of the relevant literature on quality measures and tools in HRC systems. Section 3 details the methods used in this study, including the assessment of product variant complexity and human stress response, the proposed multivariate control chart approach, and the performance evaluation of control charts and the management of system alerts. Section 4 describes the application of the proposed approach in the HRC assembly of custom electronic boards, including the monitoring of process and product defects, assembly and quality control time, and human stress levels. Section 5 presents and discusses the results obtained from the implementation of the proposed approach highlighting its robustness in detecting out-of-control situations and achieving the goals of human-centred, sustainable and resilient manufacturing in the Industry 5.0 paradigm. Finally, Section 6 draws conclusions and discusses the implications of the proposed approach for quality control in HRC

systems are also discussed, as well as its potential for extension to other process and human-related parameters.

2 Literature Review

Human-Robot Collaboration (HRC) systems have gained significant attention in recent years due to their potential to increase productivity, flexibility, and safety in manufacturing processes [11, 12]. With the growing trend of mass customization, HRC systems offer the ability to combine human skills with the precision and accuracy of collaborative robots, resulting in more efficient and effective production systems [13, 14].

To ensure optimal performance of these systems, it is important to monitor a variety of parameters, including both process and human factors. According to the scientific literature, performance measures in HRC can be categorized into four key areas: time behavior, process measures, physiological measures, and human-robot physical measures [15]. Parameters in these categories, such as response times, task completion, workspace design, safety, product quality, and the physiological state of human operators, are vital for a comprehensive understanding of HRC systems. The inclusion of these diverse measures facilitates a monitoring approach that not only focuses on the performance-centered aspects of HRC systems but also emphasizes the human-centered elements, reflecting the dual nature of these applications [16–18].

Building on this understanding, the importance of monitoring human performance parameters in HRC systems gains additional emphasis. Recent years have seen a growing focus on the impact of human factors on both performance and operator well-being within these systems. Studies exploring the design of HRC tasks have delved into the physical and cognitive aspects impacting human operators [15, 19], as well as the potential hazards associated with high-load robots [20]. Objective physiological measures, such as heart rate variability (HRV) and electrodermal activity (EDA), are increasingly used to assess how robot movements affect the operator's state during HRC tasks [21–24]. For instance, Kulić and Croft [25] showed that proximity and speed of the robot can significantly affect mental stress, while Arai et al. [26] demonstrated the impact of robot movements on EDA. Moreover, emotional and cognitive aspects have been found to be critical for HRC efficiency [27]. Thus, monitoring human parameters such as HRV and EDA is not just vital for the system's performance but is also imperative for ensuring the well-being of operators in HRC systems.

Previous studies have explored the use of Statistical Process Control (SPC) tools, such as control charts, to monitor various aspects of manufacturing processes [28, 29]. However, traditional SPC methods often focus solely on

process-related variables, neglecting the importance of human-related factors in HRC systems [15, 30]. Multivariate Control Charts (MCCs) are a more sophisticated form of SPC that can be used to monitor multiple variables simultaneously and detect any out-of-control situations [9, 31, 32]. MCCs have been applied to various fields, including manufacturing, healthcare, and finance, among others [33–38]. However, the use of MCCs in HRC systems to monitor both process and human performance parameters is relatively new and requires further investigation.

In recent years, several studies have proposed the use of MCCs for monitoring multiple variables in manufacturing processes. For example, Ahsan et al. [34] proposed a method for monitoring variable and attribute quality characteristics through MCCs based on Principal Component Analysis (PCA) Mix. An example of application was the monitoring of a one-year basis machine, and the process failure information was recorded in terms of 16 variable characteristics and three attribute characteristics. Similarly, Rodrigues et al. [33] proposed the use of MCCs to monitor the dimensional stability of a metal-mechanical process by considering multiple process variables. Harris et al. [38] used MCCs to monitor metal cutting processes, specifically titanium alloy milling, i.e. a machining process used in the manufacture of aircraft landing gear. However, to the best of our knowledge, no previous studies have investigated the use of MCCs for monitoring both process and human performance parameters in HRC systems.

In this study, a novel diagnostic method based on MCCs is proposed for real-time monitoring of HRC systems. This method aims to fill the gap in the literature by developing a diagnostic tool that considers both process and human factors. By monitoring both process performance (i.e., process total defects, assembly and quality control times) and human well-being parameters (i.e., human stress response), the proposed approach has the potential to contribute to the advancement of HRC systems to achieve human-centred, sustainable and resilient manufacturing in the Industry 5.0 paradigm.

3 Methods

This section delineates the proposed methodology for monitoring various parameters during the assembly of product variants in HRC systems, focusing on those with different complexity levels. In Section 3.1, a method to assess product variant complexity is presented. During the assembly of each product, real-time data on human and process performance parameters, including assembly and quality control times, total defects, and human stress response, are collected for monitoring. The calculation of the stress indicator is detailed in Section 3.2, while other parameters are directly acquired

during the process observation. Monitoring of these parameters via Multivariate Control Charts (MCCs) is discussed in Section 3.3. Finally, Section 3.4 introduces a performance assessment of the proposed control charts and discusses its implication for real-time management of system alerts.

It should be noted that, in the proposed approach utilizing MCCs, four parameters are monitored concurrently, i.e. assembly time, quality control time, total defects, and operator stress, without assigning any weight. However, if needed, weights could be integrated into the MCC methodology to prioritize certain parameters over others. Various weighting schemes may be used, such as the use of eigenvectors in principal component analysis or assigning different cost factors to different types of parameters [39, 40]. Such adaptations could help in situations where trade-offs between process performance and operator well-being become necessary, enabling a quantifiable balance tailored to specific operational goals or industry standards.

3.1 Product Variants Complexity

Human and process performance parameters to be monitored during the production process are highly affected by the kind of product to be manufactured and, in particular, its complexity, as demonstrated in previous studies [41]. In the present paper, each product is characterised by a certain level of complexity using the structural complexity model [42]. Based solely on structural aspects of the product, this model is easily applicable in the early stages of product design, when subjective data perceived by operators are not readily available nor robust [41]. The model, developed for manual assembly, can be extended to HRC assembly contexts, where the robot primarily performs organizational and logistical tasks such as selecting parts to be assembled in a predetermined sequence and feeding them to a human operator, in charge of manual assembly operations. In the model, structural complexity C is defined as [42]:

$$C = C_1 + C_2 \cdot C_3 \quad (1)$$

where C_1 , C_2 and C_3 represent parts, connections, and topological complexity, respectively.

C_1 is the sum of parts complexities, denoting the technical difficulty associated with managing and interacting with the product parts in isolated conditions. Among the various methods used in the literature, parts complexity can be estimated with the Lucas Method, i.e. a Design For Assembly (DFA) approach, to derive a normalised handling index [43]. This index is calculated based on the physical factors of size, weight, handling difficulties and orientation (alpha and beta symmetry).

C_2 , i.e., the complexity of connections, is the sum of the complexities of pairwise connections existing in the product

structure. Connections complexities can be estimated by the normalised fitting index from the Lucas Method [43]. The fitting index predicts the difficulty of an assembly fitting by penalising the physical attributes, including part placing, part fastening (e.g., self-securing, screwing, riveting, bending, mechanical deformation, soldering or welding, adhesive), fitting direction, visibility, alignment, and resistance to insertion, that affect the fitting difficulty.

C_3 , the topological complexity related to the architectural pattern of the assembled product, is defined as the average of singular values of the adjacency matrix of the product; it increases as the system topology shifts from centralised to more distributed architectures [42].

3.2 Human Stress Response Assessment

Numerous studies have focused on evaluating human well-being in work environments, often using physiological measures to objectively assess workers' internal states, such as heart rate variability, blood pressure, and electrodermal activity [44–47]. Understanding the mental and physical state of operators during HRC is vital for supporting their well-being. Besides feedback from self-assessment tools, physiological measures provide real-time information about the operator's state, including unconscious reactions [46, 48]. Concepts like mental workload, stress, demand, strain, and fatigue are key to understanding cognitive and psychophysical aspects in HRC. These aspects have traditionally been assessed through tools like NASA-TLX (Task Load Index) and Subjective Workload Assessment Technique (SWAT), but such tools may suffer from retrospective bias and are not suited for continuous monitoring [49–51]. Thus, physiological measures, increasingly used for comprehending the operator's state, offer a valuable alternative [45, 52]. In this study, ElectroDermal Activity (EDA) data is used as a stress indicator, evaluating average Skin Conductance Response (SCR) during HRC assembly tasks [44], as shown in Fig. 1.

To account for variations in human behavior and individual operator differences, a calibration phase was implemented for each operator before the assembly tasks. This phase involved baseline measurements under resting conditions to establish a personalized reference for each individual's stress response.

EDA data was processed using the web-based tool EDA Explorer [54]. Physiological data were first analysed to detect and remove noise and artefacts by classification algorithms. Then, Continuous Decomposition Analysis (CDA) [55] was performed to decompose the EDA signal into continuous tonic and phasic activity signals. Tonic activity, referring to long-term fluctuations in EDA not specifically elicited by external stimuli, is best characterized by changes in Skin Conductance Level (SCL). Phasic activity refers

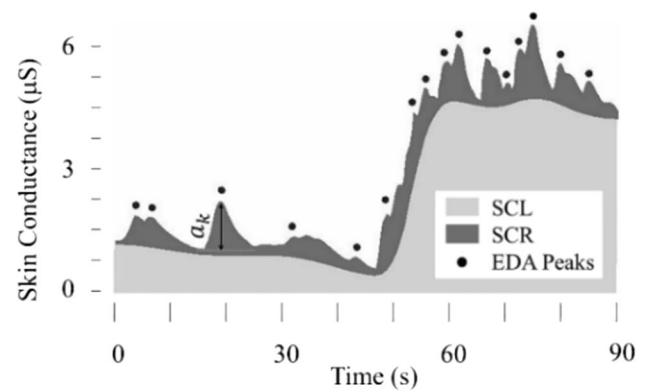


Fig. 1 Example of EDA signal during HRC assembly, adapted from [53]

instead to short-term fluctuations in EDA elicited by a usually identified and externally presented stimulus. Through the analysis of the phasic activity signal, Skin Conductance Responses (SCRs), i.e., amplitude changes from the SCL to a peak of the response (see Fig. 1), can be identified [44, 56]. In the proposed methodology, the average value of SCR peak amplitudes used as a stress indicator of each operator in assembling each product variant due to its common use [44, 56]. This metric was selected due to its sensitivity in reflecting acute stress responses in real-time, aligning with the objectives of the study.

To account for individual physiological variability, this study normalizes the peak amplitude values in the stress indicator calculation [56]. Normalization adjusts for each operator's unique stress response, ensuring that the stress indicators are comparable across individuals. As a result, the stress indicator SI obtained for each operator can be expressed as follows:

$$SI = \left[\frac{\left(\frac{\sum_{k=1}^{N_p} a_k}{N_p} \right) - a_{min}}{a_{max} - a_{min}} \right] \cdot 100 \quad (2)$$

where a_k is the amplitude of the k -th SCR peak, N_p is the total number of SCR peaks during the assembly of a certain product variant, a_{min} and a_{max} are, respectively, the minimum and maximum amplitude of SCR peaks obtained directly from the EDA signal during the assembly by each operator.

3.3 Multivariate Control Charts

The issue of monitoring human and process performance parameters can be addressed as a process monitoring problem in the SPC framework. For each individual variable, univariate control charts can be created [31], with the drawback however of not identifying out-of-control data if the

variables are correlated, as shown in Fig. 2. Thus, MCCs are to be preferred over univariate control charts for simultaneously monitoring process location and process variability of selected parameters.

Univariate control of mean and scatter is typically performed using *X-bar* and *S* control charts [31]. The *X-bar* chart monitors the process mean or average, while the *S* chart tracks the process variability or standard deviation. Their multivariate extensions are, respectively, Hotelling T^2 and Generalized Variance control charts [57], which are used for similar purposes in contexts involving multiple variables. These MCCs work well when the number of system variables is not high (10 or less) and, although being based on the assumption of normality of variable distributions, are also robust in the presence of significant deviations from this assumption [31]. However, if severe departures from normality occur and data are very skewed, a data transformation can be adopted to correct the nonnormal condition, e.g. a Box-Cox transformation [58].

Typically, two steps are included in the implementation of control charts. In Phase I, charts are used to determine if the process is in control, and the data gathered is utilised to estimate the control limits. In Phase II, charts are used to determine if the process remains in control when more data are drawn using the estimated control limits obtained in Phase I [31].

Monitoring of human and process performance parameters refers to individual observations, with one value only for each parameter being obtained for each custom product. Indeed, products are typically not produced in batches, but are often one-of-a-kind products manufactured in variable mix based on customer demand. Thus, specific values of the control limits for individual observations should be considered for the adopted charts. In detail, in Phase I, the Hotelling T^2 statistic can be approximated using a Beta distribution with parameters $\frac{p}{2}$ and $\frac{f-p-1}{2}$ [57]:

$$T^2 \sim \frac{(m-1)^2}{m} \cdot \text{Beta}\left(\frac{p}{2}, \frac{f-p-1}{2}\right) \tag{3}$$

with

$$f = \frac{2 \cdot (m-1)^2}{3 \cdot m - 4} \tag{4}$$

where p is the number of system variables and m is the number of samples used for chart construction in Phase I. Therefore, the lower control limit (*LCL*) and the upper control limit (*UCL*) are the values of T^2 statistics in Eq. (3) corresponding to a cumulative probability of 0.135% and 99.865% (corresponding to mean value -3 and +3 standard deviations for a normal distribution); however, *LCL* is typically set to zero since any shift in the mean results in an increase in T^2 .

The use of the Beta distribution in Eq. (3) is valid only in Phase I. In Phase II, the Hotelling T^2 statistics can be approximated by a Fisher distribution with parameters p and $m-p$ [57]:

$$T^2 \sim \frac{p \cdot (m+1) \cdot (m-1)}{m^2 - m \cdot p} \cdot F(p, m-p) \tag{5}$$

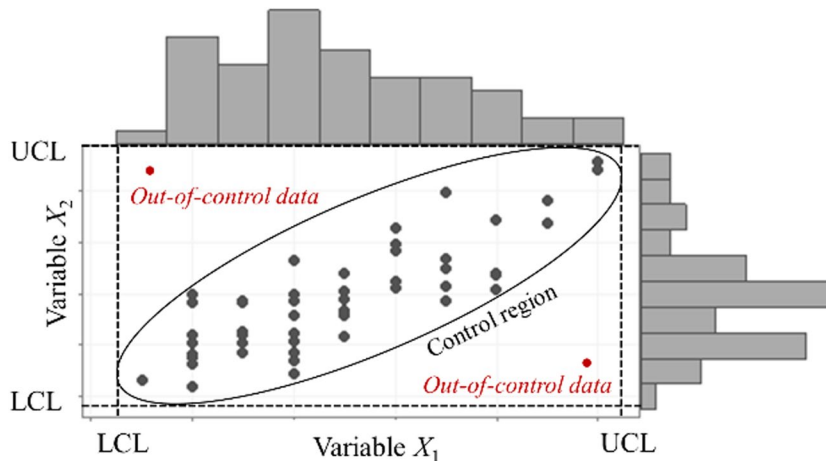
Therefore, *UCL* is now the value of T^2 statistics in Eq. (5) corresponding to a cumulative probability of 99.865% and *LCL* is set to zero.

In contrast, when using the Generalized Variance chart with individual observations, conventional formulas are not applicable and an ad-hoc procedure must be employed [31, 59]. All values should first be standardized using Sullivan and Woodall's special covariance matrix [59]:

$$S^* = \frac{1}{2 \cdot (m-1)} \sum_{i=1}^{m-1} e_i^2 \tag{6}$$

where e_i are the differences between successive observations:

Fig. 2 Marginal plot for two variables X_1 and X_2 showing out-of-controls data detected only by a multivariate approach



$$e_i = x_{i+1} - x_i \quad i = 1, \dots, m - 1 \quad (7)$$

Then, an S chart can be used, in which each subgroup corresponds to each replication [57]. Therefore, the General Variance control limits are:

$$LCL = s_m - 3 \cdot \frac{s_m}{c_4} \cdot \sqrt{1 - c_4^2} \quad UCL = s_m + 3 \cdot \frac{s_m}{c_4} \cdot \sqrt{1 - c_4^2} \quad (8)$$

where s_m is the average of the standard deviations of each subgroup and c_4 is the bias correction of the standard deviation estimate [31]. A central line corresponding to s_m is typically shown in the Generalized Variance chart. For the Generalized Variance charts, the calculation of control limits in Phase I and Phase II is the same.

3.4 Performance Evaluation of Control Charts and Management of System Alerts

A critical aspect in the assessment of control charts, such as the Hotelling T^2 and Generalized Variance charts, is their statistical performance, which can be effectively measured through the Average Run Length (ARL) [31]. The ARL is a key metric that represents the expected number of samples observed before a control chart detects a specific shift in the process being monitored. This concept is pivotal in understanding the sensitivity and responsiveness of control charts to changes in process parameters.

For the Hotelling T^2 control chart, the ARL , denoted as ARL_d , is particularly important when there is a shift in the mean vector of the process parameters. This shift is quantified in terms of the Mahalanobis distance (d), which is a measure of how far the mean vector shifts in a multi-dimensional parameter space [60]. It is important to note that the covariance matrix is assumed constant during this shift. In practical terms, the ARL_d provides a measure of how many samples, on average, the T^2 chart would examine before signaling a change of a specific magnitude [36]. It is computed by considering the probability that the T^2 statistic (see Section 3.3) exceeds the Upper Control Limit (UCL) when the mean vector has shifted.

Similarly, for the Generalized Variance chart, the performance can be assessed by considering variations in the distribution of each subgroup standard deviation [36]. This shift is quantified in terms of the distortion of amplitude q of the standard deviation of each subgroup (see Section 3.3). The resulting ARL , termed ARL_q , is calculated. The ARL_q thus offers insights into the Generalized Variance chart's ability to detect shifts in process variability as distortions in the standard deviation of subgroup distributions. The calculation involves approximating the distorted standard deviation distribution as normal, especially for a large sample size m [36].

Both ARL_d and ARL_q are crucial in optimizing the design and implementation of control charts. They enable practitioners to understand and predict how quickly a chart will respond to various types of process changes, thereby aiding in making informed decisions about process monitoring and control. Through detailed analysis of these metrics, control charts can be finely tuned to balance the detection of true process shifts against minimizing false alarms, ensuring both efficacy and efficiency in process monitoring systems.

In the context of real-time monitoring, the calculation of ARL plays a pivotal role in managing system alerts, particularly in addressing the concerns of false positives or negatives. A control chart with a low ARL is highly sensitive and may trigger alerts frequently, which could lead to an increased number of false positives. Conversely, a chart with a high ARL might be less prone to false alarms but could delay the detection of actual process shifts, potentially resulting in false negatives.

By calibrating control charts to have an optimal ARL , one can effectively manage the trade-off between sensitivity and specificity of alerts. A well-tuned ARL ensures that system alerts are neither too conservative (resulting in missed detections) nor too aggressive (leading to frequent false alarms). This calibration is particularly crucial in environments where the cost of false alerts, either in terms of operational disruption or resource allocation, is significant.

A real-time process control system might include a variety of methodologies to manage alerts. These could encompass steps such as verifying the sequence of data points post-alert to distinguish genuine signals from noise, and conducting contextual analyses to ascertain the underlying causes of observed shifts. Further, such systems are often designed to dynamically adjust detection algorithm sensitivity, ensuring that the precision of the control system is maintained. This multifaceted and adaptive approach is crucial in contemporary manufacturing and production environments, which are characterized by rapid changes and the necessity for a control system that is as responsive as it is vigilant.

The overall methodology adopted by the approach proposed in this paper is summarised in Fig. 3.

4 HRC Assembly of Custom Electronic Boards

The procedure described above was implemented and tested on an HRC system for the assembly of six customized electronic boards (ID 1—ID 6) using the ARDUINO® UNO Starter Kit (see Fig. 4(a)). The kit includes both the physical components for assembling the electronic boards (listed in Table 1) and a software package for programming the microcontrollers. Table 1 reports the type and number of

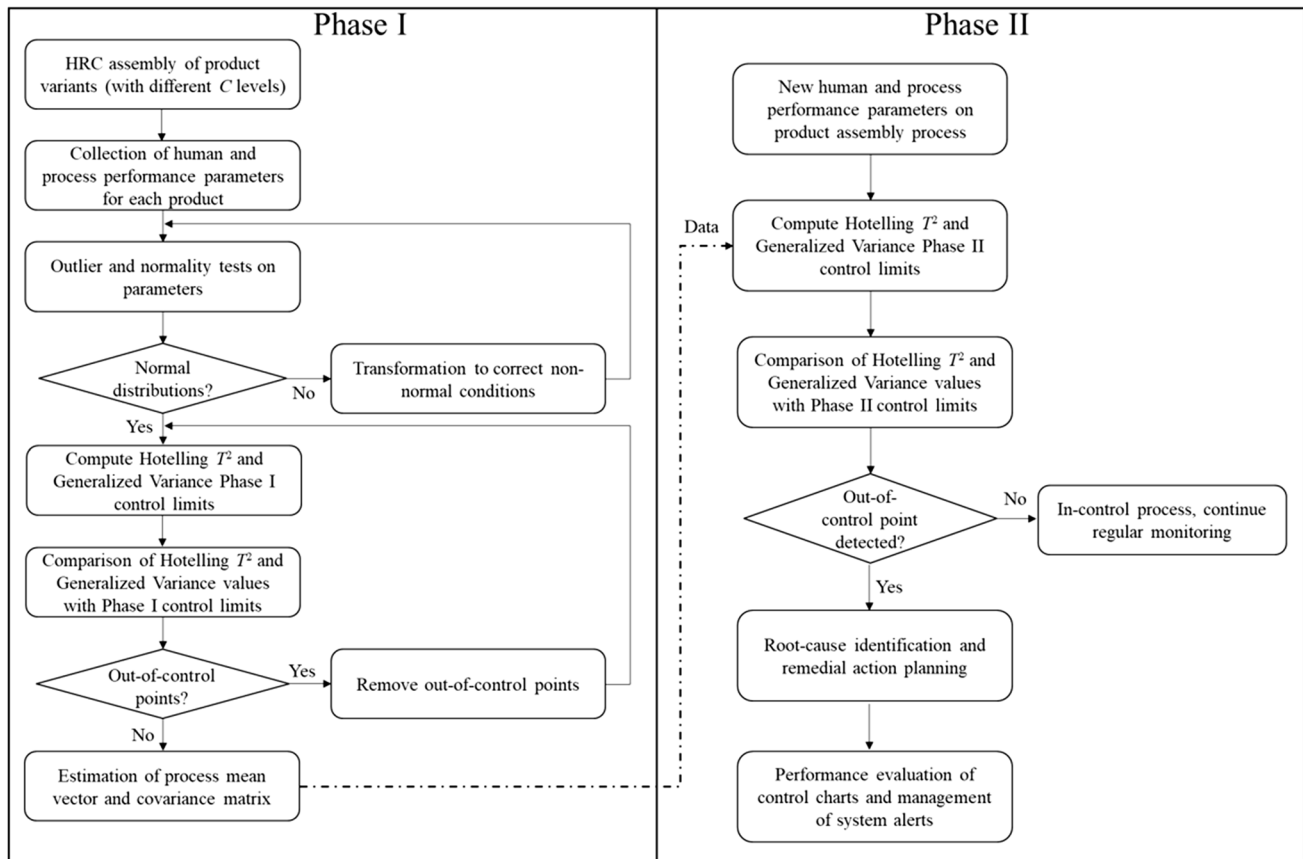
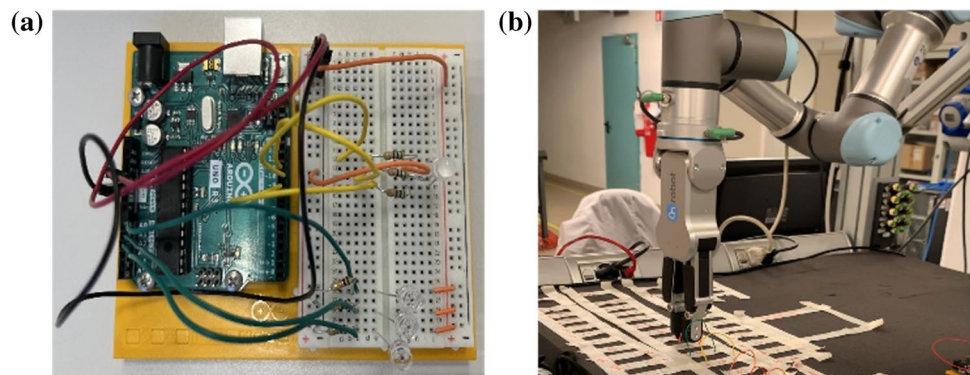


Fig. 3 Schematic of the proposed methodology

Fig. 4 (a) Example of assembled electronic board (ID 4) and (b) HRC assembly workstation



components and the complexity factors, calculated as per Section 3.1, for each electronic board. In detail,

C_1 , the handling complexity index, is derived from the Lucas method [43]. It involves aggregating scores for each component of the product, with scores assigned based on a range of factors like size, weight, handling difficulty, and orientation (including alpha and beta symmetry). Similarly, C_2 is obtained through the Lucas method [43] by summing up the difficulty values for each connection required to assemble the product. These difficulty values

are tabular scores assigned based on attributes such as component positioning and fastening, assembly direction, visibility, alignment, and resistance to insertion. Finally, C_3 is determined from the product's adjacency matrix, specifically as the mean value of the matrix's singular values [42]. For a comprehensive understanding of these complexity factors and the methodology used for their quantification, including the tables for score assignment, refer to the details provided in the specific references [43, 61].

Table 1 Characteristics of six electronic boards assembled (ID 1—ID 6)

	ID 1	ID 2	ID 3	ID 4	ID 5	ID 6
Breadboard	1	1	1	1	1	1
Long wires	-	1	2	8	9	13
Short wires	1	3	5	3	6	4
Resistors	1	1	4	6	2	2
Pushbuttons	-	2	4	-	2	1
LED	1	1	-	1	-	-
Phototransistor	-	-	-	3	-	-
Potentiometer	-	-	-	-	1	1
Piezo	-	-	1	-	-	-
LCD	-	-	-	-	-	1
Battery snap	-	-	-	-	1	-
DC Motor	-	-	-	-	1	-
N° of parts	4	9	17	22	24	23
C_1	1.64	3.12	5.35	6.59	7.49	6.97
C_2	2.90	5.89	10.03	13.39	15.83	18.24
C_3	0.75	0.57	0.45	0.40	0.37	0.39
C	3.80	6.50	9.83	11.95	13.37	14.12

Six operators (five in Phase I and one in Phase II) with experience in electromechanics and electronic circuitry, as well as automation and engineering skills, were involved in the experimental campaign. They were supported by a single-arm collaborative robot UR3e (Universal Robots™) equipped with an OnRobot RG6 flexible two-finger robot gripper (OnRobot™), as shown in Fig. 4(b). The cobot and gripper parameters used for the HRC assembly are reported in Table 2.

The cobot was used to assist operators during assembly operations with organizational and logistical tasks, by selecting and passing the correct component according to a pre-defined sequence. The human operator activated the cobot by pressing a button located near the workstation whenever it needed parts for assembly. After assembly, each electronic board was inspected by a trained quality controller to verify its operation through the software and identify any remaining defects. Operators assembled all six products in random order. For each product, the following human and process performance parameters were collected: (1) operators' physiological data using the Empatica E4 wristband (Empatica S.r.l., Milan, Italy), a non-invasive biosensor that collects EDA data at 4 Hz; (2) the number of total defects, consisting of in-process defects (*i.e.*, defects occurring during the assembly process due to both operator and cobot) and offline defects (*i.e.*, defects detected during the offline quality control); (3) assembly time

(expressed in minutes); (4) quality control time (expressed in minutes). Defects were also classified by type, such as incorrect component, misplaced component, component not picked by the cobot, component slipped by the cobot, defective component, and improperly inserted component.

5 Results and Discussion

5.1 Multivariate Control Charts Results

Multivariate control charts were exploited to monitor the four human and process performance parameters related to each product variant assembly described in Section 4. The $p=4$ system variables is an adequate number for the application of Hotelling T^2 and Generalized Variance control chart [31].

In Phase I, a total of thirty products was assembled by five operators in random order, following the experimental system configuration as per Section 4. The human and process performance parameters were collected for each product and are reported in Table 3.

All the considered variables resulted to be significantly correlated with product assembly complexity (p -value < 0.005). In detail, Pearson correlation

Table 2 Cobot and gripper parameters used in the HRC assembly

Tool	Joint speed [°/s]	Joint acc. [°/s ²]	Linear speed [mm/s]	Linear acc. [mm/s ²]	Distance [mm]	Force [N]
Cobot	200	200	200	200	-	-
Gripper	-	-	-	-	16	80

Table 3 Experimental data on human and process performance parameters

Sample no	Phase	Product	Assembly time [min]	Quality control time [min]	Total defects	Stress
1	I	ID 4	12.12	2.08	3	8.97
2	I	ID 6	14.17	5.18	7	34.87
3	I	ID 1	2.80	0.15	0	0.00
4	I	ID 5	11.13	4.03	5	10.00
5	I	ID 3	6.57	1.93	3	4.02
6	I	ID 2	2.97	0.93	1	3.13
7	I	ID 5	13.10	3.50	4	12.70
8	I	ID 4	9.00	1.10	3	16.65
9	I	ID 3	6.50	2.08	3	8.46
10	I	ID 6	14.25	1.70	5	20.45
11	I	ID 2	3.30	0.15	0	0.33
12	I	ID 1	1.32	0.15	0	0.00
13	I	ID 3	10.20	0.15	0	8.95
14	I	ID 6	17.48	2.13	6	23.27
15	I	ID 1	1.37	0.15	0	0.00
16	I	ID 4	10.03	0.30	3	12.16
17	I	ID 2	4.98	1.05	2	2.23
18	I	ID 5	13.15	0.15	3	11.30
19	I	ID 2	3.37	0.15	2	7.35
20	I	ID 4	8.85	0.15	3	14.90
21	I	ID 1	1.57	0.15	0	0.00
22	I	ID 3	6.57	0.15	0	6.35
23	I	ID 6	11.83	0.15	4	19.84
24	I	ID 5	9.28	0.15	6	11.45
25	I	ID 1	1.75	0.00	0	0.00
26	I	ID 3	5.83	0.15	2	11.12
27	I	ID 5	8.85	0.15	3	9.21
28	I	ID 6	10.43	2.42	5	22.01
29	I	ID 4	5.78	0.15	0	11.55
30	I	ID 2	1.98	0.15	1	5.00
31	II	ID 6	23.73	2.27	6	27.88
32	II	ID 6	30.00	2.31	8	50.00
33	II	ID 2	6.97	0.15	0	1.04
34	II	ID 5	14.80	0.15	1	17.31
35	II	ID 1	1.89	0.13	0	20.00
36	II	ID 3	8.22	0.15	1	8.75
37	II	ID 1	2.53	0.15	0	0.00
38	II	ID 4	11.35	0.15	2	7.75
39	II	ID 2	3.93	5.00	5	3.18

coefficients (ρ) were calculated, which measure the linear correlation between two variables. This coefficient ranges from -1 to +1, where +1 indicates a perfect positive linear correlation, 0 indicates no linear correlation, and -1 indicates a perfect negative linear correlation. The obtained values were 0.828 for stress, 0.807 for total defects, 0.910 for assembly time and 0.481 for quality control time. Figure 5 illustrates in a matrix plot the relationships between the considered variables with Pearson

correlation coefficients (ρ) and related p -values, showing strong correlation.

Obtained graphs suggest that product variant complexity is the main driver affecting the relationships among the variables.

After outlier management, the normality of variables distribution was checked by the Shapiro-Wilk test [31], resulting in the non-rejection of the normality hypothesis with a 95% confidence level. In this case study, since

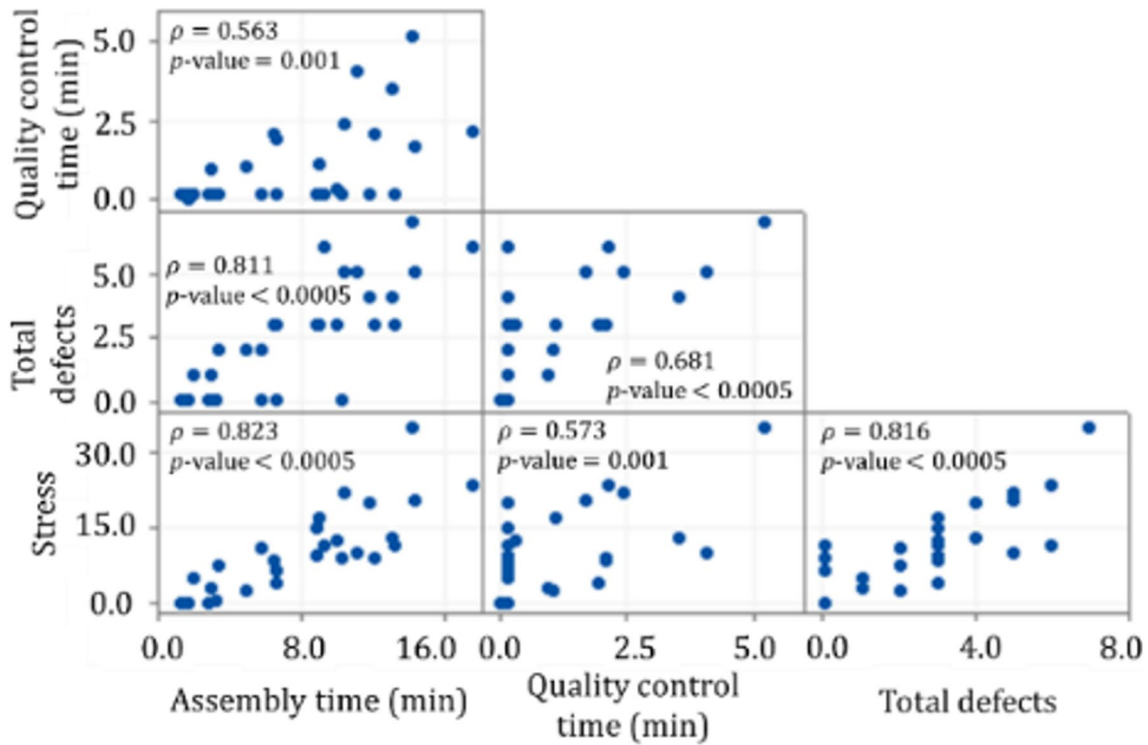


Fig. 5 Matrix plot of Phase I data with indication of Pearson correlation coefficients ρ and related p -values

the normality of the total defects distribution cannot be rejected at the 95% confidence level, the theoretical Poisson distribution can be approximated by a Gaussian distribution [31]. However, when a multiattribute and multivariable process needs to be monitored and the multivariate normal distribution is not verified, some transformation methods can be used to estimate the transformed mean vector and covariance matrix and then design the control charts [62]. For example, Niaki and Abbasi [63, 64] proposed a method for monitoring multiattribute processes based on transforming multiattribute data so that their marginal probability distributions have almost zero skewness. Simulated data were used to find the power of the (proper) root transformation for each attribute. Then, the transformed covariance matrix was estimated and used to design Hotelling T^2 control chart [63] and χ^2 control chart [64], which assumed a multivariate normal distribution, making the proposed method an approximate rather than an exact procedure.

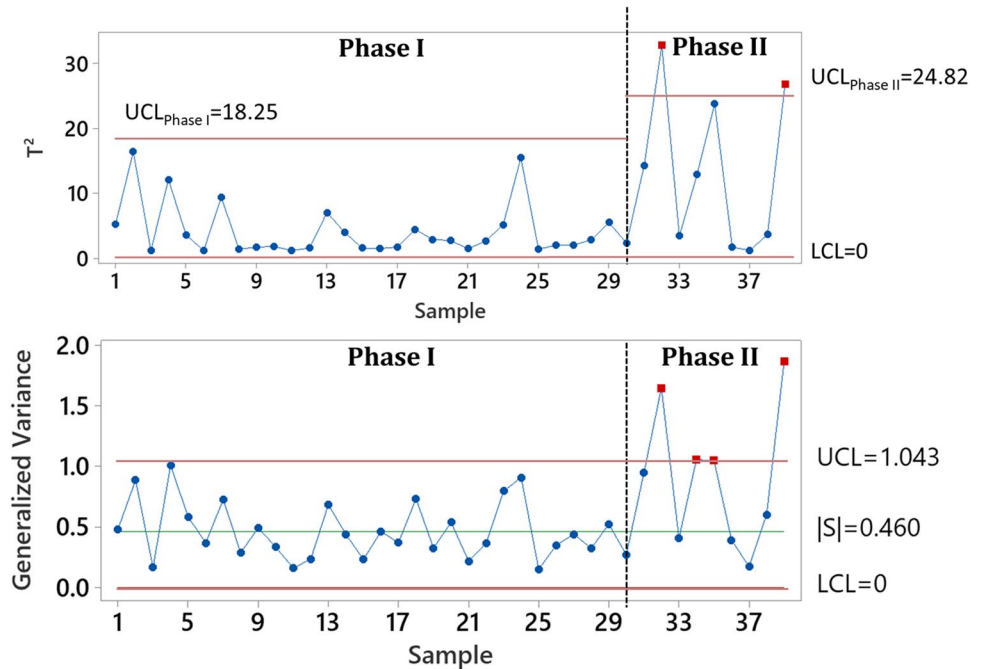
After normality tests, the data represented in Fig. 5 were used to create a historical dataset and design the control charts in Phase I (see Fig. 6). Hotelling T^2 and Generalized Variance values of Phase I are reported in Table 4, obtained by Eq. (3) and (6), respectively. The control limits of Hotelling T^2 and Generalized Variance charts of Phase I represented in Fig. 6 were obtained from Eq. (3) and (8), respectively.

As shown in Fig. 6, no out-of-control data were detected in Phase I. Accordingly, the estimates of process mean vector and covariance matrix were used in Phase II to test whether the process remained in control under normal working conditions. In Phase II, the assembly of 9 additional custom electronic boards was performed by an additional operator in random order, and the related parameters were collected, as shown in Table 3. The values of Hotelling T^2 and Generalized Variance of Phase II are reported in Table 4, obtained by Eq. (5) and (6), respectively. The control limits of Hotelling T^2 and Generalized Variance charts of Phase II represented in Fig. 6 were obtained from Eqs. (5) and (8), respectively. As shown in Fig. 6, in such a phase, two out-of-control data were detected by Hotelling T^2 chart and four points were detected by Generalized Variance chart.

In detail, to interpret out-of-control points signalled by Hotelling T^2 chart of Fig. 6 and test the significance of variables contribution to the composite value of each point, the T^2 statistic can be decomposed [65]. Accordingly, root causes can be promptly identified, as reported in Table 5, and assignable causes of variations can be removed.

In addition to the high variability detected for the samples n. 32 and n. 39, which were also identified as out-of-control points by the Hotelling T^2 chart, the Generalized Variance chart flagged samples n. 34 and n. 35 as critical. Specifically, sample n. 34 is signalled as out-of-control due to high assembly time and stress response values and low

Fig. 6 Hotelling T^2 and Generalized Variance charts for HRC assembly of custom electronic boards (Phase I calibration data and Phase II new data)



total defects, while sample n. 35 is signalled as out of control due to high stress response values.

5.2 Comparison with Univariate Control Charts

This section delves into the comparison between the outcomes obtained from the MCC method proposed in this paper and those derived from univariate control charts. The aim is to highlight the differences in results due to the lack of consideration for the correlations between variables when employing univariate control charts.

For the analysis, univariate control charts were utilized for each variable as follows [31]:

- Assembly time, Quality control time and Stress: an I-MR (Individuals and Moving Range) chart was used, suitable for continuous data that are normally distributed when each sample consists of a single measurement.
- Total defects: a c-chart was used, appropriate for counting defects when each sample is a single unit.

Table 6 encapsulates the findings from univariate control charts. In detail, Table 6 reports the type of control chart used for each variable, the calculated control limits, the out-of-control points identified in Phase II, and the specific control chart (Individual or Moving Range for the first three variables, and c-chart for the fourth variable) where the outliers were identified. The Upper Control Limit (UCL) and Lower Control Limit (LCL) for these charts were calculated using data from Phase I (see Table 3).

In contrast to the results from the Hotelling T^2 chart and Generalized Variance chart discussed in Section 5.1, the univariate control charts identified out-of-control points at samples 31 and 38, indicating a deviation from the expected range for specific variables. However, these points do not align with the out-of-control samples (32 and 39) identified by the Hotelling T^2 chart and samples (32, 34, 35, and 39) identified by the Generalized Variance chart.

The disparity in results between univariate and multivariate approaches is notable. The univariate approach, while effective in signaling deviations in individual variables, fails to capture the complex interrelations and the collective behavior of the variables due to neglecting the correlations among them. This discrepancy highlights the enhanced sensitivity of the MCC method, which can detect subtle shifts in the process that might be overlooked by univariate charts. In contrast, the MCC method, through the Hotelling T^2 chart and Generalized Variance chart, offers a comprehensive analysis by considering the correlations and interdependencies among variables. This is particularly crucial in complex manufacturing processes where multiple variables interact and influence each other.

The difference in the number of out-of-control points detected by the two methods also underscores this point. The MCC method, by accounting for the correlations between variables, is able to identify a broader set of potential issues, suggesting its suitability for complex process monitoring where understanding the interplay between variables is key. In contrast, the univariate method, while simpler and more straightforward, might be more suited for processes where

Table 4 Hotelling T^2 and Generalized Variance values in Phase I and Phase II

Sample no	Phase	Product	Hotelling T^2	Generalized Variance
1	I	ID 4	5.28	0.479
2	I	ID 6	16.44	0.883
3	I	ID 1	1.22	0.166
4	I	ID 5	12.09	1.005
5	I	ID 3	3.60	0.581
6	I	ID 2	1.22	0.367
7	I	ID 5	9.41	0.722
8	I	ID 4	1.41	0.286
9	I	ID 3	1.75	0.491
10	I	ID 6	1.83	0.332
11	I	ID 2	1.20	0.159
12	I	ID 1	1.61	0.234
13	I	ID 3	7.07	0.682
14	I	ID 6	4.00	0.438
15	I	ID 1	1.58	0.231
16	I	ID 4	1.51	0.461
17	I	ID 2	1.76	0.369
18	I	ID 5	4.45	0.731
19	I	ID 2	2.92	0.323
20	I	ID 4	2.75	0.537
21	I	ID 1	1.49	0.217
22	I	ID 3	2.67	0.366
23	I	ID 6	5.18	0.793
24	I	ID 5	15.50	0.905
25	I	ID 1	1.43	0.150
26	I	ID 3	2.03	0.348
27	I	ID 5	2.05	0.439
28	I	ID 6	2.86	0.322
29	I	ID 4	5.54	0.521
30	I	ID 2	2.33	0.270
31	II	ID 6	14.27	0.942
32	II	ID 6	32.84	1.641
33	II	ID 2	3.46	0.405
34	II	ID 5	12.88	1.052
35	II	ID 1	23.78	1.045
36	II	ID 3	1.72	0.390
37	II	ID 1	1.24	0.171
38	II	ID 4	3.66	0.599
39	II	ID 2	26.84	1.858

Table 5 Out-of-control data summary for Hotelling T^2 chart (Phase II)

Sample	Product variant	Main root-cause variables (p -value)	Out-of-control reason
32	ID 6	Stress (0.0105), Total defects (0.0279), Assembly time (0.0296)	Defective product components detected in-process by operator
39	ID 2	Quality control time (0.0012), Stress (0.0151)	Wrong/faulty components undetected by the operator during production process

variables operate more independently or where the primary concern is monitoring individual process metrics.

5.3 Performance Evaluation of the Control Charts

The performance of the Hotelling T^2 control chart has been evaluated by calculating ARL_d for Phase I through simulation for different values of Mahalanobis distance d [60]. It has been assumed that all parameters have a normal distribution and, given a specific value of d , all their averages vary by the same percentage W . The obtained results are shown in Table 7.

By applying the same procedure for Phase II, similar results are obtained.

Similarly, performance of the Generalized Variance chart has been evaluated through simulation by considering a distortion of amplitude q of the distribution of the standard deviation. By varying the value q , the results shown in Table 8 are obtained.

The results highlighted in Tables 7 and 8 demonstrate the robust statistical performance of the Hotelling T^2 and Generalized Variance control charts, respectively, as determined through simulation processes. For both charts, there is a clear inverse correlation between the ARL metrics (ARL_d for the T^2 and ARL_q for the Generalized Variance) and the respective distortion parameters (Mahalanobis distance d and amplitude q). These findings corroborate the expected behavior that as the extent of deviation or distortion increases, the control charts' sensitivity to detecting shifts also rises, hence the observed decrease in ARL values. Such behavior emphasizes the charts' agility in signaling significant deviations, reinforcing their utility in continuous process monitoring. The recalibrated values within these tables are indicative of a vigilant and adaptive monitoring system, tailored to maintain high operational quality while minimizing the likelihood of false detections.

6 Conclusions

Human-Robot Collaboration (HRC) systems are currently used in the production of custom products due to their inherent precision and accuracy in assisting and complementing human skills. To ensure optimal system performance, several process and human parameters must be

Table 6 Out-of-control data summary for Univariate Control Charts (Phase II)

Variable	Chart Type	Central Line	<i>UCL</i> (Upper Control Limit)	<i>LCL</i> (Lower Control Limit)	Out-of-control points (Phase II)	Control Chart Type for Outliers
Assembly time [min]	I-MR	7.68 min	24.33 min	0 min	31	I
Quality control time [min]	I-MR	1.03 min	4.11 min	0 min	38	I
Stress	I-MR	9.88	39.08	0	31	I
Total defects	c	2.47	7.18	0	31	c

Table 7 ARL_d of the Hotelling T^2 chart for different values of the Mahalanobis distance d obtained by assuming that all the p parameters have a normal distribution and all their averages vary of the same percentage W

d	0.75	1	2	3	4	5	6
W	0.45%	0.6%	1.2%	1.8%	2.4%	3.0%	3.6%
ARL_d	350.2	220.4	48.3	12.7	5.1	2.6	1.3

Table 8 ARL_q of the Generalized Variance chart for different values of the amplitude q of the distortion of the distribution of the standard deviation

q	1.0	1.2	1.4	1.6	1.8	2.0
ARL_q	358.7	52.4	15.8	7.1	3.9	2.3

jointly monitored within the production system. In the production of a range of custom product variants, high correlations between system's parameters are often found due to the varying levels of product assembly complexity. To address this, a novel diagnostic approach for detecting variations in process performance and human parameters in HRC is proposed, involving using multivariate control charts, i.e., Hotelling T^2 for mean and Generalized Variance for variability, to jointly monitor HRC parameters. An innovative aspect of the proposed approach is the combined monitoring of process performance and human-related factors, which are rarely considered in statistical process control. By relying on real-time data collected during production, this method allows for quick and comprehensive stability control at both the product/process and human levels. The identification of out-of-control situations caters for the achievement of goals for human-centric, sustainable, and resilient manufacturing in the Industry 5.0 paradigm.

In addition, the proposed method can be easily integrated into HRC software or a digital twin for quality control without requiring additional procedures, making it highly adaptable and scalable to different manufacturing settings. The robustness of the method has been demonstrated in HRC assembly of custom electronic boards, where defectiveness, assembly and quality control time, and human stress levels were monitored.

Furthermore, the proposed method has the potential to be extended to other parameters related to process performance, such as costs and sustainability measures, as well as other human-related aspects, such as Heart Rate Variability (HRV) indicator [44]. This will enable manufacturers to monitor and optimize multiple aspects of their production processes, resulting in increased productivity, efficiency, and quality of the system, while also ensuring the well-being of operators. The flexibility of the proposed MCC-based diagnostic approach, with its ability to integrate various types of data, makes it highly scalable and adaptable to larger production systems and diverse industries. Its modular design allows for the easy inclusion of additional parameters, supporting its application in varied manufacturing contexts beyond custom electronic board assembly.

Author Contributions All authors contributed to the study conception and design. Material preparation, data collection and analysis were performed by Stefano Puttero and Elisa Verna. Gianfranco Genta and Maurizio Galetto verified the analytical methods and supervised the findings of this work. The first draft of the manuscript was written by Elisa Verna and all authors commented on previous versions of the manuscript. All authors read and approved the final manuscript.

Funding Open access funding provided by Politecnico di Torino within the CRUI-CARE Agreement. The authors declare that no funds,

grants, or other support were received during the preparation of this manuscript.

Code Availability Data cannot be openly shared to protect the privacy of study participants.

Declarations

Ethics Approval The authors respect the Ethical Guidelines of the Journal.

Consent to Participate Informed consent was obtained from all individual participants included in the study.

Consent to Publish Not applicable.

Competing Interests The authors have no relevant financial or non-financial interests to disclose.

Open Access This article is licensed under a Creative Commons Attribution 4.0 International License, which permits use, sharing, adaptation, distribution and reproduction in any medium or format, as long as you give appropriate credit to the original author(s) and the source, provide a link to the Creative Commons licence, and indicate if changes were made. The images or other third party material in this article are included in the article's Creative Commons licence, unless indicated otherwise in a credit line to the material. If material is not included in the article's Creative Commons licence and your intended use is not permitted by statutory regulation or exceeds the permitted use, you will need to obtain permission directly from the copyright holder. To view a copy of this licence, visit <http://creativecommons.org/licenses/by/4.0/>.

References

- ElMaraghy, H., Schuh, G., ElMaraghy, W., Piller, F., Schönsleben, P., Tseng, M., Bernard, A.: Product variety management. *CIRP Ann.* **62**, 629–652 (2013)
- Faccio, M., Minto, R., Rosati, G., Bottin, M.: The influence of the product characteristics on human-robot collaboration: a model for the performance of collaborative robotic assembly. *Int. J. Adv. Manuf. Technol.* **106**, 2317–2331 (2020)
- Verna, E., Genta, G., Galetto, M., Franceschini, F.: Planning offline inspection strategies in low-volume manufacturing processes. *Qual. Eng.* **32**, 705–720 (2020)
- Slamanig, M., Winkler, H.: An exploration of ramp-up strategies in the area of mass customisation. *Int. J. Mass Cust.* **4**, 22–43 (2011)
- Shoval, S., Efatmaneshnik, M.: Managing complexity of assembly with modularity: a cost and benefit analysis. *Int. J. Adv. Manuf. Technol.* **105**, 3815–3828 (2019)
- Partanen, J., Haapasalo, H.: Fast production for order fulfillment: Implementing mass customization in electronics industry. *Int. J. Prod. Econ.* **90**, 213–222 (2004)
- Krüger, J., Lien, T.K., Verl, A.: Cooperation of human and machines in assembly lines. *CIRP Ann.* **58**, 628–646 (2009)
- Verna, E., Genta, G., Galetto, M., Franceschini, F.: Zero defect manufacturing: a self-adaptive defect prediction model based on assembly complexity. *Int. J. Comput. Integr. Manuf.* **36**, 155–168 (2023)
- Hotelling, H.: Multivariate quality control. In: Eisenhart, C., Hastay, M., and Wallis, W.A. (eds.) *Techniques of Statistical Analysis*. pp. 111–184. McGraw-Hill, New York, NY (1974)
- Verna, E., Puttero, S., Genta, G., Galetto, M.: Toward a concept of digital twin for monitoring assembly and disassembly processes. *Qual. Eng.* (2023). <https://doi.org/10.1080/08982112.2023.2234017>
- Bauer, A., Wollherr, D., Buss, M.: Huma-robot collaboration: a survey. *Int. J. Humanoid Robot.* **5**, 47–66 (2007)
- Galín, R., Mamchenko, M.: Human-robot collaboration in the society of the future: a survey on the challenges and the Barriers. In: *Futuristic Trends in Network and Communication Technologies: Third International Conference, FTNCT 2020, Taganrog, Russia, October 14–16, 2020, Revised Selected Papers, Part I 3*. pp. 111–122. Springer, Singapore (2021)
- Gervasi, R., Mastrogiacomo, L., Franceschini, F.: A conceptual framework to evaluate human-robot collaboration. *Int. J. Adv. Manuf. Technol.* **108**, 841–865 (2020)
- Inkulu, A.K., Bahubalendruni, M.V.A.R., Dara, A.: Challenges and opportunities in human robot collaboration context of Industry 4.0-a state of the art review. *Ind. Robot Int. J. Robot. Res. Appl.* **49**, 226–239 (2022)
- Coronado, E., Kiyokawa, T., Ricardez, G.A.G., Ramirez-Alpizar, I.G., Venture, G., Yamanobe, N.: Evaluating quality in human-robot interaction: a systematic search and classification of performance and human-centered factors, measures and metrics towards an industry 5.0. *J. Manuf. Syst.* **63**, 392–410 (2022)
- European Commission, Directorate-General for Research and Innovation, Breque, M., De Nul, L., Petridis, A.: *Industry 5.0: Towards a sustainable, human-centric and resilient European industry*, Publications Office of the European Union (2021). <https://data.europa.eu/doi/10.2777/308407>
- Leng, J., Sha, W., Wang, B., Zheng, P., Zhuang, C., Liu, Q., Wuest, T., Mourtzis, D., Wang, L.: Industry 5.0: Prospect and retrospect. *J. Manuf. Syst.* **65**, 279–295 (2022)
- Xu, X., Lu, Y., Vogel-Heuser, B., Wang, L.: Industry 4.0 and Industry 5.0—Inception, conception and perception. *J. Manuf. Syst.* **61**, 530–535 (2021). <https://doi.org/10.1016/J.JMSY.2021.10.006>
- Colim, A., Faria, C., Cunha, J., Oliveira, J., Sousa, N., Rocha, L.A.: Physical ergonomic improvement and safe design of an assembly workstation through collaborative robotics. *Safety*. **7**, 14 (2021)
- Khalid, A., Kirisci, P., Ghrairi, Z., Thoben, K.D., Pannek, J.: Towards implementing safety and security concepts for human-robot collaboration in the context of Industry 4.0. In: *39th International MATADOR Conference on Advanced Manufacturing*. pp. 55–63 (2017)
- Argyle, E.M., Marinescu, A., Wilson, M.L., Lawson, G., Sharples, S.: Physiological indicators of task demand, fatigue, and cognition in future digital manufacturing environments. *Int. J. Hum. Comput. Stud.* **145**, 102522 (2021)
- Bradley, M.M., Lang, P.J.: Measuring emotion: the self-assessment manikin and the semantic differential. *J. Behav. Ther. Exp. Psychiatry* **25**, 49–59 (1994)
- Gervasi, R., Barravecchia, F., Mastrogiacomo, L., Franceschini, F.: Applications of affective computing in human-robot interaction: State-of-art and challenges for manufacturing. *Proc. Inst. Mech. Eng. Part B J. Eng. Manuf.* **237** (6-7), 815–832 (2022)
- Gervasi, R., Aliev, K., Mastrogiacomo, L., Franceschini, F.: User experience and physiological response in human-robot collaboration: a preliminary investigation. *J. Intell. Robot. Syst.* **106**, 36 (2022)
- Kulic, D., Croft, E.A.: Affective state estimation for human-robot interaction. *IEEE Trans. Robot.* **23**, 991–1000 (2007)

26. Arai, T., Kato, R., Fujita, M.: Assessment of operator stress induced by robot collaboration in assembly. *CIRP Ann.* **59**, 5–8 (2010)
27. Galin, R.R., Meshcheryakov, R.V.: Human-robot interaction efficiency and human-robot collaboration. In: Kravets, A.G. (ed.) *Robotics: Industry 4.0 Issues & New Intelligent Control Paradigms*, pp. 55–63. Springer International Publishing, Cham (2020)
28. Bahria, N., HarbaouiDrirdi, I., Chelbi, A., Bouchriha, H.: Joint design of control chart, production and maintenance policy for unreliable manufacturing systems. *J. Qual. Maint. Eng.* **27**, 586–610 (2021)
29. Verna, E., Genta, G., Galetto, M., Franceschini, F.: Defects-per-unit control chart for assembled products based on defect prediction models. *Int. J. Adv. Manuf. Technol.* **119**, 2835–2846 (2022)
30. Damacharla, P., Javaid, A.Y., Gallimore, J.J., Devabhaktuni, V.K.: Common metrics to benchmark human-machine teams (HMT): a review. *IEEE Access.* **6**, 38637–38655 (2018)
31. Montgomery, D.C.: *Introduction to statistical quality control*. John Wiley & Sons, New York (2019)
32. Montgomery, D.C., Wadsworth, H.M.: Some techniques for multivariate qualitycontrol applications. *Trans ASQC.* **26**, 427–435 (1972)
33. Rodrigues, D.C., Goecks, L.S., Mareth, T., Korzenowski, A.L.: Multivariate control chart with variable dimensions for flexible production environments. *Int. J. Qual. Res.* **15**, 701 (2021)
34. Ahsan, M., Mashuri, M., Kuswanto, H., Prastyo, D.D., Khusna, H.: Multivariate control chart based on PCA mix for variable and attribute quality characteristics. *Prod. Manuf. Res.* **6**, 364–384 (2018)
35. Lowry, C.A., Montgomery, D.C.: A review of multivariate control charts. *IIE Trans.* **27**, 800–810 (1995)
36. Franceschini, F., Galetto, M., Genta, G.: Multivariate control charts for monitoring internal camera parameters in digital photogrammetry for LSDM (Large-Scale Dimensional Metrology) applications. *Precis. Eng.* **42**, 133–142 (2015)
37. Suman, G., Prajapati, D.: Control chart applications in healthcare: a literature review. *Int. J. Metrol. Qual. Eng.* **9**, 5 (2018)
38. Harris, K., Triantafyllopoulos, K., Stillman, E., McLeay, T.: A multivariate control chart for autocorrelated tool wear processes. *Qual. Reliab. Eng. Int.* **32**, 2093–2106 (2016)
39. Cornford, S.L., Gibbel, M.: *Methodology for physics and engineering of reliable products*, Wescon/96, Anaheim, USA, October 22–24, pp. 618–624 (1996)
40. Li, S., Xiong, X.: Multi-response robust design based on principal component and grey relational analysis, *Proceeding of the 11th World Congress on Intelligent Control and Automation*, Shenyang, China, 29 June - 04 July, pp. 5024–5029 (2014).
41. Verna, E., Genta, G., Galetto, M., Franceschini, F.: Defect prediction for assembled products: a novel model based on the structural complexity paradigm. *Int. J. Adv. Manuf. Technol.* **120**, 3405–3426 (2022)
42. Sinha, K.: *Structural complexity and its implications for design of cyber-physical systems*. PhD Thesis. Massachusetts Institute of Technology (2014)
43. Alkan, B., Vera, D., Ahmad, B., Harrison, R.: A method to assess assembly complexity of industrial products in early design phase. *IEEE Access.* **6**, 989–999 (2017)
44. Gervasi, R., Aliev, K., Luca, M., Franceschini, F.: User experience and physiological response in human-robot collaboration: a preliminary investigation. *J. Intell. Robot. Syst.* **106**, 1–30 (2022)
45. Argyle, E.M., Marinescu, A., Wilson, M.L., Lawson, G., Sharples, S.: Physiological indicators of task demand, fatigue, and cognition in future digital manufacturing environments. *Int. J. Hum. Comput. Stud.* **145**, 102522 (2021). <https://doi.org/10.1016/J.IJHCS.2020.102522>
46. Arai, T., Kato, R., Fujita, M.: Assessment of operator stress induced by robot collaboration in assembly. *CIRP Ann.* **59**, 5–8 (2010). <https://doi.org/10.1016/J.CIRP.2010.03.043>
47. Körner, U., Müller-Thur, K., Lunau, T., Dragano, N., Angerer, P., Buchner, A.: Perceived stress in human-machine interaction in modern manufacturing environments—results of a qualitative interview study. *Stress Heal.* **35**, 187–199 (2019). <https://doi.org/10.1002/SML.2853>
48. Verna, E., Puttero, S., Genta, G., Galetto, M.: exploring the effects of perceived complexity criteria on performance measures of human-robot collaborative assembly. *J. Manuf. Sci. Eng.* **145**, (2023). <https://doi.org/10.1115/1.4063232/1166422>
49. Marinescu, A.C., Sharples, S., Ritchie, A.C., Sánchez López, T., McDowell, M., Morvan, H.P.: Physiological parameter response to variation of mental workload. *Hum. Factors* **60**, 31–56 (2018). https://doi.org/10.1177/0018720817733101/ASSET/IMAGES/LARGE/10.1177_0018720817733101-FIG2.JPEG
50. Reid, G.B., Nygren, T.E.: The subjective workload assessment technique: a scaling procedure for measuring mental workload. *Adv. Psychol.* **52**, 185–218 (1988). [https://doi.org/10.1016/S0166-4115\(08\)62387-0](https://doi.org/10.1016/S0166-4115(08)62387-0)
51. Hart, S.G., Staveland, L.E.: Development of NASA-TLX (Task Load Index): Results of empirical and theoretical research. In: Hancock, P.A., Meshkati, N. (eds.) *Advances in Psychology*, pp. 139–183. Elsevier, North-Holland (1988)
52. Charles, R.L., Nixon, J.: Measuring mental workload using physiological measures: a systematic review. *Appl. Ergon.* **74**, 221–232 (2019). <https://doi.org/10.1016/J.APERGO.2018.08.028>
53. Geršak, G., Drnovšek, J.: Electrodermal activity patient simulator. *PLoS ONE* **15**, e0228949 (2020)
54. Taylor, S., Jaques, N., Chen, W., Fedor, S., Sano, A., Picard, R.: Automatic identification of artifacts in electrodermal activity data. In: 2015 37th Annual International Conference of the IEEE Engineering in Medicine and Biology Society (EMBC). pp. 1934–1937. IEEE (2015)
55. Benedek, M., Kaernbach, C.: A continuous measure of phasic electrodermal activity. *J. Neurosci. Methods* **190**, 80–91 (2010)
56. Zhao, B., Wang, Z., Yu, Z., Guo, B.: EmotionSense: Emotion recognition based on wearable wristband. In: 2018 IEEE SmartWorld, Ubiquitous Intelligence & Computing, Advanced & Trusted Computing, Scalable Computing & Communications, Cloud & Big Data Computing, Internet of People and Smart City Innovation (SmartWorld/SCALCOM/UIC/ATC/CBDCOM/IOP/SCI). pp. 346–355. IEEE (2018)
57. Tracy, N.D., Young, J.C., Mason, R.L.: Multivariate control charts for individual observations. *J. Qual. Technol.* **24**, 88–95 (1992)
58. Osborne, J.W.: Improving your data transformations: applying the Box-Cox transformation. *Pract. Assess. Res. Eval.* **15**, 1–9 (2010)
59. Sullivan, J.H., Woodall, W.H.: A comparison of multivariate control charts for individual observations. *J. Qual. Technol.* **28**, 398–408 (1996)
60. Mahadik, S.B.: Hotelling’s T₂ charts with variable control and warning limits. *Int. J. Qual. Eng. Technol.* **3**, 158–167 (2012)
61. Verna, E., Puttero, S., Genta, G., Galetto, M.: A novel diagnostic tool for human-centric quality monitoring in human-robot collaboration manufacturing. *J. Manuf. Sci. Eng.* **145**, (2023). <https://doi.org/10.1115/1.4063284/1166536>
62. Topalidou, E., Psarakis, S.: Review of multinomial and multiattribute quality control charts. *Qual. Reliab. Eng. Int.* **25**, 773–804 (2009)
63. Niaki, S.T.A., Abbasi, B.: Skewness reduction approach in multiattribute process monitoring. *Commun. Stat. Methods.* **36**, 2313–2325 (2007)
64. AkhavanNiaki, S.T., Abbasi, B.: On the monitoring of multi-attributes high-quality production processes. *Metrika* **66**, 373–388 (2007)

65. Mason, R.L., Tracy, N.D., Young, J.C.: Decomposition of T2 for multivariate control chart interpretation. *J. Qual. Technol.* **27**, 99–108 (1995)

Publisher's Note Springer Nature remains neutral with regard to jurisdictional claims in published maps and institutional affiliations.

Elisa Verna received the Master of Science Degree in Industrial Engineering and Management in 2016 and the PhD in Management, Production and Design in 2021 from Politecnico di Torino. She is currently Assistant Professor at the Department of Management and Production Engineering (DIGEP) of the Politecnico di Torino. She is Fellow of A.I.Te.M. and E.N.B.I.S. (European Network for Business and Industrial Statistics). Her current research interests are Quality Engineering and Management, Statistical Process Control and Innovative Production Systems.

Stefano Puttero received the Master of Science Degree in Industrial Engineering and Management in 2021 from Politecnico di Torino. He is currently a PhD student at the Department of Management and Production Engineering (DIGEP) of the Politecnico di Torino. He is Fellow of A.I.Te.M. (Associazione Italiana delle Tecnologie Manifatturiere). His current research interests are Quality Engineering, Defect Detection and Human-Robot Collaboration. In particular, he is focusing on the study, implementation and planning of innovative quality

inspection procedures in different manufacturing processes, and on the development of defect generation models in manual and human-robot collaborative assembly and disassembly processes.

Gianfranco Genta received the Master of Science Degree in Mathematical from Politecnico di Torino in 2005 and the PhD Degree in Metrology: Measuring Science and Technique from Politecnico di Torino in 2010. He is currently Associate Professor at the Department of Management and Production Engineering (DIGEP) of the Politecnico di Torino. He is Research Affiliate of CIRP (The International Academy for Production Engineering) and Fellow of A.I.Te.M. He is author and co-author of three books and more than 70 publications on national/international journals and conference proceedings. His current research focusses on Industrial Metrology, Quality Engineering and Experimental Data Analysis.

Maurizio Galetto received the Master of Science degree in Physics from University of Turin, Italy, in 1995 and the PhD Degree in Metrology: Measuring Science and Technique from Politecnico di Torino in 2000. He is currently Head of Department and Full Professor at the Department of Management and Production Engineering (DIGEP) of the Politecnico di Torino. He is Associate Member of CIRP and Fellow of A.I.Te.M. and E.N.B.I.S. He is author and co-author of four books and more than 100 publications on scientific journals and conference proceedings. His current research interests are Quality Engineering, Statistical Process Control and Industrial Metrology.